JOURNAL OF BACTERIOLOGY, Jan. 1988, p. 422–430
0021-9193/88/010422-09$02.00/0

Vol. 170, No. 1

Rate and Topography of Cell Wall Synthesis during the Division Cycle of *Salmonella typhimurium*

STEPHEN COOPER

Department of Microbiology and Immunology, University of Michigan Medical School, Ann Arbor, Michigan 48109-0620

Received 9 January 1987/Accepted 14 August 1987

The rates of synthesis of peptidoglycan and protein during the division cycle of *Salmonella typhimurium* have been measured by using the membrane elution technique and differentially labeled diaminopimelic acid and leucine. The cells were labeled during unperturbed exponential growth and then bound to a nitrocellulose membrane by filtration. Newborn cells were eluted from the membrane with fresh medium. The radioactivity in the newborn cells in successive fractions was determined. As the cells are eluted from the membrane as a function of their cell cycle age at the time of labeling, the rate of incorporation of the different radioactive compounds as a function of cell cycle age can be determined. During the first part of the division cycle, the ratio of the rates of protein and peptidoglycan synthesis was constant. During the latter part of the division cycle, there was an increase in the rate of peptidoglycan synthesis relative to the rate of protein synthesis. These results support a simple, bipartite model of cell surface increase in rod-shaped cells. Before the start of constriction, the cell surface increased only by cylindrical extension. After cell constriction started, the cell surface increased by both cylinder and pole growth. The increase in surface area was partitioned between the cylinder and the pole so that the volume of the cell increased exponentially. No variation in cell density occurred because the increase in surface allowed a continuous exponential increase in cell volume that accommodated the exponential increase in cell mass. Protein was synthesized exponentially during the division cycle. The rate of cell surface increase was described by a complex equation which is neither linear nor exponential.

There have been many measurements of the rate of cell wall synthesis during the division cycle (25, 38, 54, 60, 64, 69), and although they differ in detail, they have generally arrived at similar results. There is a continuous increase in the rate of surface synthesis during the division cycle, with some reports of peaking in the rate of synthesis near the end of the division cycle. Much of the theoretical analysis of these results has been directed toward distinguishing among simple mathematical descriptions of synthesis such as exponential or linear growth patterns or combinations of these (3, 14, 15, 20, 31, 35, 38, 39, 53, 55–59, 61–63, 70, 72, 73). In addition, the rate of surface synthesis during the division cycle has been determined by measuring the size and shape of growing cells and deriving the rules of cell growth and the rate of cell surface synthesis from these distributions (7, 12, 21, 24, 29, 45, 51–53).

The rate and mode of cell wall synthesis during the division cycle of a gram-negative rod-shaped bacterium has now been reinvestigated by measuring the rate of incorporation of diaminopimelic acid and leucine during the division cycle of *Salmonella typhimurium*. There is evidence that the modes of growth for different cells of the gram-negative rod-shaped group (e.g., *Salmonella* and *Escherichia* spp.) are similar (66). This allows the work performed here on *Salmonella* spp. to be related to other work on *Escherichia coli*. A number of years ago, we demonstrated that the division cycle events of *S. typhimurium* could be analyzed by the membrane elution technique. At that time, the pattern of DNA replication during the division cycle was analyzed (11). Another reason *S. typhimurium* was chosen for this study was the finding that incorporation of diaminopimelic acid into *S. typhimurium* is much more efficient than incorporation into *E. coli* (10), the organism used in most of the earlier studies. Compared with *S. typhimurium*, *E. coli* is relatively impermeable to diaminopimelic acid, even in diaminopimelic acid-requiring strains.

The experiments and analysis described here were stimulated by the experiments and mathematical analysis of Woldringh et al. (71). They demonstrated, using refined autoradiographic techniques, a decrease in the rate of cell wall synthesis in the cylindrical portion of the cell after cell constriction starts. Their mathematical analysis proposed an exponentially increasing increment in the total amount of cell wall synthesis during the constriction period to make up for the deficit of surface area synthesized before constriction. Evidence is presented here for the constant relative rate of increase of surface area to mass increase during the preconstriction period. I propose a model for the partition of wall syntheses between the pole and lateral wall during the constriction period. This model is consistent with the constant density of the cell and explains the decrease in the rate of cylinder extension in constricting cells. The pattern of synthesis of the cell wall, while simple to describe, is not represented by any of the simple mathematical patterns that have been considered as possible candidates for cell wall synthesis.

MATERIALS AND METHODS

Bacterial strains. *S. typhimurium* 2616 (LT7 *lys*) was obtained from Kenneth E. Sanderson of the University of Calgary, Calgary, Alberta, Canada. It is 30 to 50 times more efficient at incorporating diaminopimelic acid than a number of *E. coli* strains examined (10). Diaminopimelic acid added to this strain labels peptidoglycan exclusively.

Membrane elution method. Medium C (22) (6 g of Na_2HPO_4, 3 g of KH_2PO_4, 2 g of NH_4Cl, 3 g of NaCl, and 0.25 g of $MgSO_4$ per liter) supplemented with 0.2% glycerol

and 40 μg of lysine per ml was used throughout. The bacteria were grown at 37°C with rotary shaking for at least 15 h before the start of an elution experiment. Exponentially growing cells were labeled with [^{3}H]diaminopimelic acid and [^{14}C]leucine for approximately 5% of the generation time (2 to 4 min for cells with a doubling time of 60 min). The cells were filtered on a nitrocellulose membrane (Millipore Corp., Bedford, Mass.; GSWP), and the filter was washed with prewarmed medium and inverted. Fresh warm medium was then pumped through the membrane. After an initial release of unbound and loosely bound cells, the eluate contained only newborn cells released from the membrane by cell division (8, 11, 22, 23). A fraction of each sample was taken for a cell count with a Coulter counter. A larger fraction (4 to 5 ml) was taken for the determination of the amounts of diaminopimelic acid and leucine incorporated. Since the initial washing on the membrane removed unincorporated radioactivity, the eluted material was counted without filtration. Control experiments indicated that there was no significant pool of unincorporated material in the cells eluted from the membrane.

In the experiments presented below, the ratios of incorporation of different labels were studied in the cells eluted from the membrane. Various rises and falls in this ratio were interpreted in support of a particular model of cell surface growth. The question thus arises as to whether the results are reproducible and statistically reliable. In experiments (unpublished) with *E. coli* and *S. typhimurium* with *N*-acetylglucosamine as a label for cell wall, the results reported here with diaminopimelic acid have been confirmed. Further, tritiated leucine and carbon-labeled leucine gives a ratio that is a flat line (standard deviation of 1%; maximum deviation of 3%) when plotted (see Fig. 3 and 4). These results indicate that the variations in the ratios when leucine and diaminopimelic acid are the labels are not due to some artifact of the labeling or analysis method. This experiment also shows that the results are statistically valid, since the reconstruction experiment, with differentially labeled leucine, was done with the same number of cell and radioactivity counts that were present in the experiments presented here.

Radioactivity sources and measurements. [^{14}C]leucine (450 μCi/mmol) was purchased from New England Nuclear Corp., Boston, Mass. The [^{3}H]*meso*-diaminopimelic acid (36.5 Ci/mmol) was from Research Products International, Mount Prospect, Ill. Scintillation fluids which are compatible with water (Safety Solve; Research Products International) allowed the counting of up to 5 ml of eluate without filtration of the cells. A Beckman 3801 scintillation counter (Beckman Instruments, Inc., Fullerton, Calif.) was used to count the samples; this instrument corrected for quench in different samples. The counts were also automatically corrected for spillover of the tritium and carbon labels into the alternate windows.

A comment on the methodology. Can one make a choice as to the proper methodology for investigating biosynthetic patterns during the division cycle? The method used here has had a major success, and the model of DNA synthesis which was derived using this methodology (9) has been confirmed by an entirely independent methodology (65). I therefore suggest that the membrane elution method is a suitable candidate for revealing the rate of cell surface and mass synthesis during the division cycle.

The model. The basis for the model of cell surface increase is a rod-shaped gram-negative bacterial cell that is approximated as a right circular cylinder capped with two hemispheres (Fig. 1, age 0). The cell age, α, of a cell during the division cycle is 0.0 for a newborn cell and 1.0 for a cell at division. Electron microscopic evidence indicates that invagination of rod-shaped cells does not begin until later in the division cycle (4, 37, 39, 71). In the first part of the division cycle, before constriction starts, growth of the cell surface occurs only by extension and elongation of the cylindrical lateral wall (Fig. 1, ages 0.0 to 0.5). For any extension of the cylinder to produce a given increment of volume, for a constant cell diameter during the division cycle (1, 49; see, however, reference 67), there is a corresponding increment of surface area relative to that increase in volume. The increments of surface and volume are shown in Fig. 1 as contiguous sectors inserted into the cylinder, but the insertion is actually diffuse and not localized as suggested by Koch et al. (28, 36) on theoretical grounds and experimentally by others (46, 60, 68, 71). Before constriction starts, for each increment in cell volume there will be a corresponding

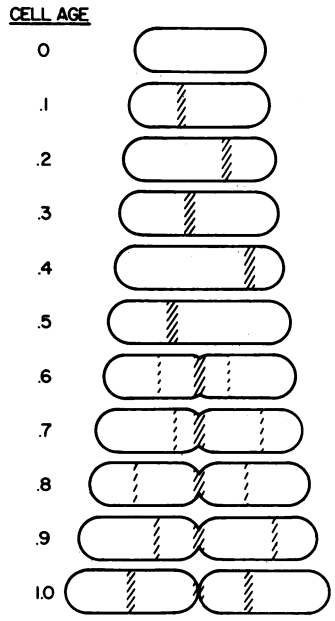

FIG. 1. Illustration of the proposed model of cell growth. Newborn cells have a cylinder length (L) of 2 and a radius (r) of 0.5. Before invagination, growth of the cell proceeds only by cylinder growth. The shaded regions in the cell indicate the amount and location (whether in the pole or the cylinder) of extension since the previous cell. The width of the shaded area is drawn to scale. It should be considered that cell growth is occurring throughout the cylinder and not in a narrow contiguous band. Each shaded sector indicates the increase in volume (ΔV) and surface area (ΔA). During cylinder growth, the ratio of these two factors is constant. When pole synthesis starts (at age α of 0.5 in the cells illustrated here), there is an increase in volume and area in the region of the new poles. Any volume increase, determined by the increase in mass, that is not accommodated by new poles is accommodated by additional cylinder growth. Cylinder growth after constriction starts is slower than before constriction. This is schematically illustrated by the thinner sector in the expanding side wall immediately after the start of constriction. As the new pole increases, in increments of equal area between the indicated ages, the volume accommodated by the new poles is continuously decreasing. Therefore, the growth rate in the cylindrical portion increases continuously during the constriction period. At the end of the division cycle the rate of synthesis in the cylinder is the same as the rate for a newborn cell. There is no sharp change in the rate of cylinder elongation at the instant of division.

increment in the cell surface in the cylinder, and for a cell with a constant radius, the ratio of cell area to cell volume increase will be constant. This relationship is independent of the mode of increase of cell volume, whether by linear, exponential, bilinear, or other means.

When invagination and constriction start, the rates of volume and area increase are no longer proportional. This is seen by considering that the surface area enclosing a unit of volume in a spherical pole is greater than the surface lateral wall area enclosing that unit volume in a cylindrical portion of a cell. Considering only the increase in the new pole volume, the first sector of volume (closest to the cylinder) has less area extended per unit volume increase than the last volume of pole extension at the tip of the hemispherical pole (Fig. 1; compare age 0.6 to age 1.0). During pole synthesis, the ratio of the rate of surface area increase to the rate of cell volume or mass increase is greater than the ratio before constriction starts.

For a newborn cell, the actual increase in the above ratios depends on three factors. The first factor is the age during the division cycle when constriction starts. The second factor is the initial shape of the cells which determine what fraction of the total surface is pole, and the third factor is the presumed mode of increase of the polar hemispheres. I have assumed that poles are synthesized with a constant rate of increase in surface area. Woldringh et al. (71) assumed an exponentially increasing pole area during constriction. Their model proposes that the synthesis of pole area begins slowly and then increases at a time when the area remaining to be synthesized is continuously decreasing. An alternate model would propose that the pole area is synthesized in proportion to the circumference at the leading edge of the pole-growing area. Synthesis would start out high at the start of constriction and decrease as the diameter of the growing area at the pole decreased. The model used here, pole growing with equal areas per unit time, is somewhere between those models.

Not discussed in the model of Woldringh et al. is how new cell wall synthesis is partitioned between the new pole and the lateral wall during the constriction period. This is a central concern of the proposal of this paper. The model proposed below assumes that after pole synthesis starts, whatever remains of the increased volume that is not accommodated by the volume increase in new pole is accommodated by an increase in the volume of the cylindrical portion of the cell. An analogy would be that new pole increase is a pressure relief system which relieves the stress on the side wall and so lowers the rate of cylindrical growth. These mathematical relationships are derived and summarized in the accompanying Appendix.

To summarize, the geometry of a rod-shaped cell growing with constant diameter and constant density implies that the ratio of the rate of cell wall synthesis to the rate of protein or mass synthesis will be constant before constriction starts and will increase after constriction. Experimentally, this means that the ratio of the rates of incorporation of diaminopimelic acid to leucine would be constant before constriction and would increase after constriction starts.

An example of the predicted results for a particular example is shown in Fig. 2. Figure 1 is a pictorial rendering of the results of Fig. 2 drawn to scale. Although the volume of the cell is shown to be increasing exponentially (Fig. 2b and d), the total area and the total length do not increase exponentially (Fig. 2a, c, and d). The rates of increase are quite similar to the exponential growth rates, however, and it would be very difficult to distinguish any experimental results from exponential synthesis. Figure 2d illustrates the volume and area increase on a logarithmic scale. The area increases in a manner different from that of the volume, yet the density of the cell is constant throughout the cycle. At age 0.5, there is a sharp drop in the rate of increase of the cylindrical portion of the cell, although there is no sharp drop in the total area increase. This is seen clearly in Fig. 1, where the increase in the cell surface in the region of new pole formation is approximately equal to the amount of surface that would have been synthesized if invagination had

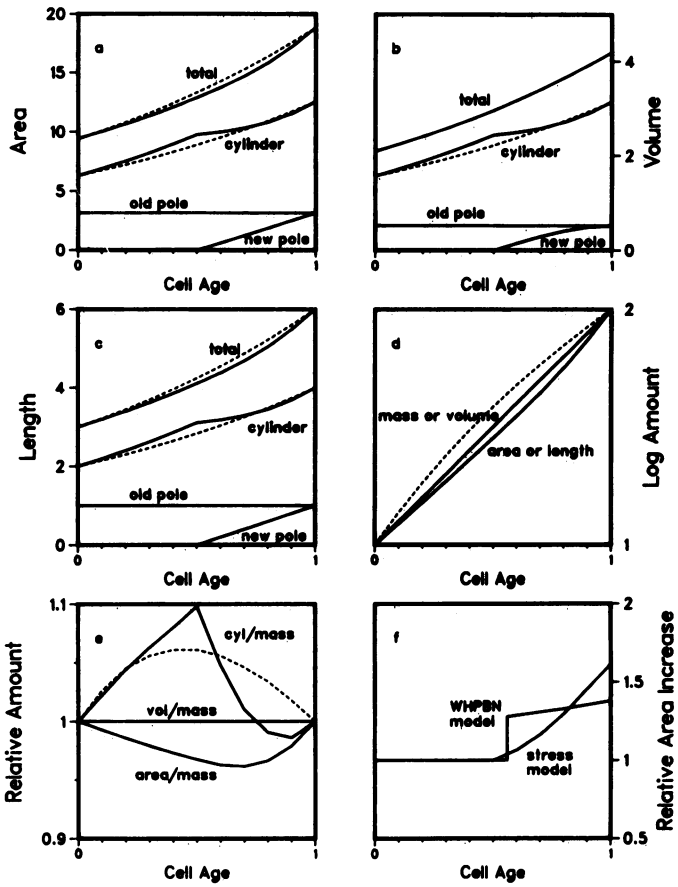

FIG. 2. Graphical illustration of the proposed model. The calculations from the equations in the text are applied to a cell with a total length of 3, a cylinder length of 2, a radius of 0.5, and with constriction starting at age 0.5 (Fig. 1). (a) Area of the new poles, old poles, cylinder, and total cell during the division cycle. The dotted line indicates the expected line for exponential synthesis of total surface, and the line associated with the cylinder is for exponential increase in the cylindrical portion of the cell. (b) Volume of the new poles, old poles, cylinder, and total cell during the division cycle. No distinction between an exponential curve and the volume increase is observed because volume increases exponentially. (c) Length of the new pole, old pole, cylinder, and total cell. (d) Increase in area, volume, length and mass plotted on a logarithmic scale. The volume and mass give a straight line and the area and length differ slightly from the exponential curve. The dotted line is the expected function for a linear increase. (e) Amount of volume, cylindrical area, and total area is divided by the mass at each time; the normalized ratio is plotted. A horizontal line indicates exponential increase. (f) Differential rate of area to mass increase. Note the slow increase in the ratio as the cell invaginates (after age 0.5). Also illustrated in Fig. 2f is the prediction of the model of Woldringh et al. (WHPBN) (71) which predicts a discontinuity in the rates of wall synthesis at the start of constriction.

not started. This is indicated by the very small amount of cylindrical growth between ages 0.5 and 0.6.

The difference between exponential or linear growth and the rate of length and area extension is shown in Fig. 2e. The scale of this figure magnifies the differences, which are quite small (Fig. 2a and c). Measurements of cell growth and length extension which demonstrate an exponential mode of increase (38, 45) are not in disagreement with this model. If cylinder length could be measured independently of total cell length, the larger deviation from exponential growth (Fig. 2e) may provide a source of experimental support for this model. Aside from this point, there is a dramatic decrease in the rate of cylinder extension (Fig. 2e) after constriction starts. This is consistent with the autoradiographic evidence (71).

In Fig. 2f, the predicted differential rate of area to mass increase is illustrated. The important point, aside from the curve itself, is that there is no sharp discontinuity in the rate of increase of cell area. No sudden change in biosynthetic capacities has to be postulated, since there is a gradual increase in the biosynthetic rate. In contrast, I have illustrated the model (the WHPBN model) of Woldringh et al. (71), which has a sharp discontinuity at the start of constriction.

Figure 2 indicates that it would be extremely difficult to distinguish the proposed rate of cell wall or cell area increase from a simple exponential increase, but it does indicate that if one normalized the results to the increase in cell mass, then one can distinguish the results of the model proposed here from a simple exponential increase in cell wall during the division cycle. If the surface and the mass both increase exponentially during the division cycle, the ratio of the incorporation rates of compounds measuring their respective syntheses would be constant. In contrast, in the model proposed here, there would be a constant ratio during the first part of the division cycle and an increase in the rate of area increase to mass increase during the latter part of the division cycle, after the start of invagination.

RESULTS

The membrane elution technique is a method for measuring the rate of synthesis of a particular macromolecule during the division cycle. Exponentially growing, unperturbed cells are labeled for a short time with a label specific for the molecule of interest. The cells are filtered onto a cellulose nitrate membrane, the membrane is inverted, and fresh medium is pumped through it. A fraction of the labeled cells bind to the membrane and grow in the presence of the medium pumped over the cells. Only newborn cells arising by division are released from the membrane. The first cells released by division arise from the oldest cells in the labeled culture, that is, those cells which were just about to divide at the time the cells were labeled. With further incubation, the newborn cells are released from cells which were increasingly younger, in terms of the division cycle, at the time of labeling. Cells are released from the membrane with label which reflects the labeling of the cells, during balanced and unperturbed growth, as a function of the division cycle. By considering cells in reverse order of elution and over one generation of elution, the rate of incorporation of a radioactive label as a function of the division cycle can be determined.

It is important that the membrane elution technique, while producing synchronized populations of cells by elution, is not a synchrony technique. The cells are labeled in unperturbed exponential growth, and analysis of the cells occurs after the label has been incorporated. Any perturbation of the cells by filtration or subsequent elution is irrelevant to the determination of the rate of incorporation of the compounds during the division cycle. All that is required of the cells on the membrane is that they divide in order and release only newborn cells into the effluent.

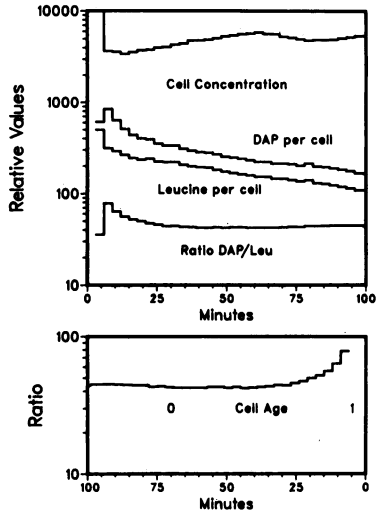

FIG. 3. Rate of incorporation of diaminopimelic acid and leucine during division cycle determined by the membrane elution technique. Fifty milliliters of cells at 2.5×10^8/ml were labeled for 3 min with 2 μCi of [^{14}C]leucine and 200 μCi of [^{3}H]diaminopimelic acid. The cells were then bound to a membrane and analyzed as described in Materials and Methods. The lower box plots the ratio in reverse. Reading from left to right, from age 0 at the time of labeling to age 1 at the time of labeling, there is a constant ratio that increases in the older cells.

Rate of peptidoglycan and protein synthesis during the division cycle. *S. typhimurium* was labeled with radioactive leucine and diaminopimelic acid and analyzed by the membrane elution technique. A typical result is presented in Fig. 3. The ratio of diaminopimelic acid to leucine started relatively high and decreased to a constant level during the first generation of elution. The same data can be considered in reverse (i.e., reading backwards from approximately 70 min on the graph) to analyze the change in the ratio as the cells progressed from young to old. The ratio was constant during the first part of the division cycle and increased toward the end of the division cycle (Fig. 3). The crests and troughs in the cell elution curve were used to identify the different generations of elution (23).

Examination of the data for the radioactivity per cell for the different labeled precursors (Fig. 3 and 4) reveals that the leucine content per cell is described by a decreasing exponential curve, whereas the diaminopimelic acid content curve has variations that lead to the observed shape of the ratio curve. The leucine curve indicates that the rate of incorporation of leucine into the cell is exponential. Therefore, the rate of synthesis of protein during the division cycle is exponential.

By themselves, the individual elution curves (diaminopimelic acid-cell and leucine-cell) are difficult to analyze and interpret because both are very close to the exponential rate. The deviations in the diaminopimelic acid curve are best understood when considering the ratio of incorporation of

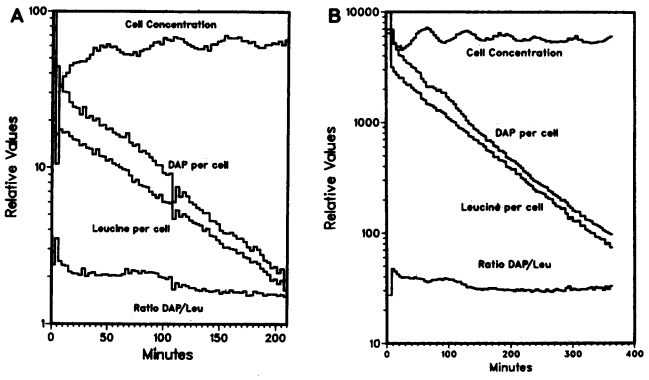

FIG. 4. Two examples of the rate of incorporation of diaminopimelic acid and leucine during the division cycle determined by the membrane elution technique. (A) Fifty milliliters of cells at 1.5 × 10^8/ml were labeled for 1 min with 2 μCi of [^{14}C]leucine and 30 μCi of [^{3}H]diaminopimelic acid and analyzed as described in Materials and Methods. (B) One hundred milliliters of cells at 2.4 × 10^8/ml were labeled for 4 min with 2 μCi of [^{14}C]leucine and 100 μCi of [^{3}H]diaminopimelic acid and analyzed as described in Materials and Methods.

diaminopimelic acid to leucine. The ratio curve fits the model described above and, in particular, the curve (stress model) in Fig 2f.

Extended elution times: analysis of the stability and segregation of peptidoglycan. Elution experiments have been carried out for up to six generations (Fig. 4A and B). After the initial decrease in the ratio of diaminopimelic acid to leucine incorporation, there was a plateau that reflects the constant ratio of surface to mass increase in the early part of the division cycle and the increased ratio in the later part of the division cycle. This plateau was then followed by a small but reproducible increase in the ratio (Fig. 4A and B). Finally, a decrease in the ratio occurred and the ratio remained constant over the next four generations. No further decrease in the ratio of diaminopimelic acid to leucine was observed. These observations are interpreted as follows. (i) The increase in the ratio after the first plateau is due to the release of cells, in the second generation, that have been labeled in the newly forming pole. While the leucine label has been decreasing by halves at each generation because of equipartition of leucine label at each division, the diaminopimelic acid is not equipartitioned at the second generation of elution. Because the label in the newly formed pole of the cell that remained attached to the membrane is completely eluted at the next division (Fig. 5), an increase is expected in the ratio of diaminopimelic acid to leucine. The rise is small, reflecting a small fraction of pole to total area. Dispersion of the cell division times also presumably precludes a clear observation of the expected rise. (ii) By the third generation, no labeled pole material remains, because of complete release of poles during the first and second generations of elution. Only label from the cylindrical portion is released during the third and subsequent generations of elution. On the average, there is a decrease in the rate of lateral wall synthesis in the latter part of the cycle (Fig. 1). This leads to the observed decrease in the diaminopimelic acid-to-leucine ratio in the third generation (Fig. 4 and 5). (iii) The constancy of the ratio with continued elution (Fig. 4) implies two important conclusions that are dealt with in detail below. One is that there is no turnover of the peptidoglycan in *S. typhimurium*. The other is that the lateral wall material is partitioned equally for at least six generations, with no preferential synthesis in any portion of the cylinder.

DISCUSSION

The rates of peptidoglycan and protein synthesis during the division cycle have been measured by the membrane elution technique. The results are consistent with a model predicting a constant ratio of the rate of cell surface increase to the rate of volume or mass increase before the start of constriction and an increase in the ratio after the start of constriction. The experiments are not able to distinguish the precise mode of new pole formation, but the results fit a model of a constant rate of pole-area increase. Throughout the cell cycle, there is no change in density, since the cell volume and the cell mass both increase exponentially.

Rate of peptidoglycan synthesis during the division cycle. This rate is a complex pattern, neither exponential nor linear (equations 2 and 3), that paradoxically is quite easy to describe. Before the start of constriction, when cylindrical extension is the only means of cell growth, the rate of peptidoglycan synthesis is similar to the differential rate of mass and volume increase. After constriction starts, the rate increases compared with mass and volume synthesis. Even if one had a perfect experimental result and exact measurements describing the rate of cell wall synthesis during the division cycle, the results would, by themselves, be unintelligible because the equation for the surface area (equations 2 and 3) is extremely complex but similar to the exponential rate. For the varying rate of cell wall synthesis to be

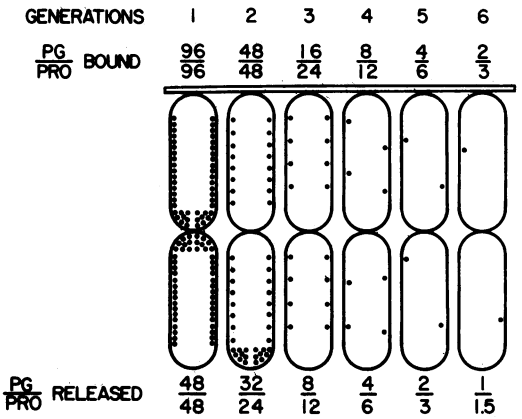

FIG. 5. Pattern of elution of protein (PRO) and peptidoglycan (PG) from pulse-labeled cells bound to a membrane. A cell in the process of forming poles and labeled with similar amounts of peptidoglycan and protein label (taken, for example, as 96 U in each case) is allowed to be eluted from the membrane. The leucine eluted in subsequent generations is halved at each generation (48, 24, 12, 6, 3, 1.5, etc.), whereas the behavior of the peptidoglycan is indicated by the dots on the periphery of the dividing cell. There are 96 dots on the first cell undergoing constriction. The poles are assumed to have 32 dots, and the walls have 64 dots. At the first division, 48 dots (or units of peptidoglycan) are released. At the next division, there is an unequal partition of the peptidoglycan as 32 U of peptidoglycan are released and 16 U remain in the membrane-bound cell. In the third generation, only lateral wall material is present and so only 16 dots are released in the third, 8 in the fourth, 4 in the fifth, and 2 in the sixth generation of elution. As the leucine is being released with different values, the ratios show an increase in the second, a decrease in the third, and constant values (with no turnover and random segregation of the side wall material) in the third, fourth, fifth, and sixth generations.

understood, the rate of wall synthesis during the division cycle must be compared with the rate of mass synthesis or volume increase.

Density of bacteria. A number of models of cell growth have invoked regulation of cell division by variations in cell density (57, 58). In contrast to those theoretical proposals, many experiments indicate that the density of *E. coli*, and by extension to a homologous organism the density of *S. typhimurium*, is invariant during the division cycle (32, 42–44, 50). The relationship of these observations to the current work can be looked at in two complementary ways. Given the constant density and the rod-shaped nature of the organism, it follows logically that the organism will grow as described in the model in Fig. 1. An alternative interpretation is that the results of the diaminopimelic acid and leucine incorporation reported here predict a constant density.

Stability and turnover of peptidoglycan. Turnover of peptidoglycan during the growth of *E. coli* has been reported (6, 18, 19). The results presented here suggest that no measurable or significant turnover of peptidoglycan, that is, a process(es) that leads to the loss of material from the cell, occurs in *S. typhimurium*. If there were turnover, one would expect to observe it readily in this experimental situation, as the cells are being continuously washed with fresh medium. Turnover in which material is rapidly reincorporated and not lost from the cell is not eliminated by these experiments. If any turnover occurs, it must be minimal and not greater than the turnover of protein in the cell. Since the bulk of the cell protein is stable in exponentially growing cells (34), this suggests that there is no measurable turnover of peptidoglycan in *S. typhimurium*. This is schematically illustrated in Fig. 5, where the expected ratios of radioactive diaminopimelic acid and leucine are calculated for a simple case for six generations. By the third generation, there is a constant ratio of the two labels, and this ratio remains constant in succeeding generations. Even without the use of a double label, the experimental results (Fig. 3 and 4) show that the half time for the decrease in the label of both the leucine and the diaminopimelic acid is the same as the generation time of the cells on the membrane. This supports the proposal that there is no measurable turnover and that both leucine (i.e., protein) and diaminopimelic acid (i.e., peptidoglycan) are subdivided equally during division of the cells on the membrane.

It may be that the difference between *E. coli* and *S. typhimurium* is because almost all experiments on turnover in *E. coli* were carried out with a diaminopimelic acid auxotroph, strain W7. *E. coli* is rather impermeable to diaminopimelic acid (10), and large amounts of diaminopimelic acid must be present in the medium to ensure growth. It is possible that the physiology of the organism is disturbed by diaminopimelic limitation. This is supported by Driehuis and Wouthers (16), who noted that limiting diaminopimelic acid led to the production of abnormal peptidoglycan.

Mode of segregation of peptidoglycan. Van Tubergen and Setlow (68) were the first to look at the segregative distribution of peptidoglycan. They noted that there was a uniform segregation pattern, indicating a large number of randomly segregated subunits. This was supported by the theoretical arguments of Koch (28) and by other experiments demonstrating a random dispersion of peptidoglycan (5, 46). Later models and experiments by Donachie and Begg (2, 13) suggested that there was a conserved unit cell mainly on the basis of studies related to the outer membrane. The results in Fig. 4 indicate that cell wall material is subdivided randomly for at least six generations. The results are consistent with a halving of the lateral wall at each division and a random distribution of material at cell division and are incompatible with the unit cell model of cell surface growth.

Rate of cell length growth. From measurements of the cell length distribution of exponentially growing cells, it was concluded that cell growth was exponential (39, 45). Figure 2c shows that the model proposed here predicts a cell length increase which is approximately exponential. Considering the limitations of those experiments, the results demonstrating exponential growth can be taken as consistent with the model proposed here.

Rate of cylinder extension. Woldringh et al. (71) noted that the incorporation of diaminopimelic acid into the lateral walls of cells with constrictions was significantly less than incorporation into the lateral walls of cells without constrictions. This unexpected observation is predicted by the proposed model (Fig. 1 and 2a, c, and e). Whereas lateral wall synthesis decreased, synthesis at the site of constriction increased (71). Woldringh et al. suggest that this increase occurs "at the expense of the activity [i.e., synthetic or growth activity] in the lateral wall." What is the mechanism of this redistribution of synthesis between the pole and the side wall? If there were a limited supply of enzymatic machinery or wall precursors available for peptidoglycan synthesis, for example, then when pole synthesis started there would be a reduction, by competition, in the rate of lateral wall synthesis. An alternative view suggests that there is no limitation in the amount of precursor for cell wall synthesis or the enzymatic machinery for cell wall synthesis. When pole synthesis starts, the increase in cell volume by pole growth relieves the stress in the cylinder area. Because of this reduction in stress, the rate of insertion of peptidoglycan in the lateral wall is reduced. This proposal, within the terms of the surface stress model, does not propose any mechanism for changing the rate of wall synthesis other than the passive one of altering the amount of stress that a particular part of the cell receives during the division cycle.

The difference between the stress model proposed here and the model of Woldringh et al. (71) is illustrated in Fig. 2f. The differential rates of peptidoglycan to mass synthesis during the cycle are compared. Although the hypothesis of Woldringh et al. predicts a discontinuity in the rate of peptidoglycan synthesis, there is no such discontinuity predicted in the model proposed here. There is a smooth transition to an increasing rate of peptidoglycan synthesis compared with the rate of mass synthesis during pole formation. Also, at division the rate of peptidoglycan synthesis is twice the initial rate of peptidoglycan synthesis; there is no sudden change in the rate of peptidoglycan synthesis even at the moment of cell division. The rate of peptidoglycan synthesis changes smoothly, with no discontinuities, either during the division cycle or between division cycles.

Surface stress model. Koch and his colleagues (27–30, 33) have proposed the surface stress model, which proposes that cell wall growth is regulated by the growth of cell mass. The results reported here support the surface stress model.

Rate of mass synthesis during the division cycle. Mass has been generally assumed to be synthesized in an exponential manner during the division cycle (17, 53), although other models such as linear (40, 42) or bilinear (41) modes of growth have been suggested. The evidence presented here (the leucine uptake curves in Fig. 3 and 4) support an exponential mode of mass or protein synthesis during the division cycle.

Explanation of anomalous shift-up results. When exponentially growing cells are suddenly placed in a richer medium, the cells are said to undergo a shift-up. Mass synthesis

changes to the new rate almost immediately, whereas cell number increase remains at the original, preshift rate for 60 (or C + D) min and then abruptly changes to the new, postshift rate (8, 26). This fundamental observation is rigorously explained by the requirement for the newly initiated rounds of DNA synthesis to pass through a constant period of replication (C min) and another constant period between termination and cell division (D min) before expressing a new rate of cell division (8, 48). It has been noted that there are minor anomalies in the shift-up, and when the differential rate of cell division is studied by the membrane elution technique, there is a temporary shortening of the D period in the extant cells immediately after the shift-up (8, 47). Some cells in the D period reach division sooner than expected, whereas those not yet in the D period have a D period of expected length.

I suggest a possible mechanism for the anomalous division after a shift-up. If one assumes that the radius of the cylinder where new pole synthesis starts is fixed at the time that invagination starts, this implies that the volume of the new pole is fixed. After a shift-up, the cell immediately changes the rate of mass synthesis to the new, faster rate. The new poles may now be expanded by the new mass more rapidly than they would have otherwise, and cells can divide earlier than they would have. To explain the normal division of cells which have not yet entered the D period at the time of shift-up, one must postulate that either there is an alteration in the starting time of the invagination process in the new medium or the effective radii of the new constrictions must change. These mechanisms would restore the constant D period found in steady-state growth in cells growing at a wide range of growth rates (9).

APPENDIX

Mathematical analysis of wall growth. In this section, an equation for the total area of a cell at any time during the division cycle will be derived. The rate of surface increase in relation to the rate of cell mass increase will also be calculated. The following assumptions will be made. (i) The rate of mass and volume increase is exponential during the division cycle. (ii) The cell density is constant during the division cycle. (iii) Constriction starts at a particular age during the division cycle. (iv) The cell can be approximated by a cylinder capped with two hemispheres. (v) The new pole grows at a constant rate of area increase after the start of constriction. (vi) Any volume increase in the cell that is not accommodated by the increase in new pole volume is accommodated by an increase in the cylindrical wall of the cell.

In the derivation, A, V, L, and r indicate the area, volume, cylindrical length, and radius of the cell, respectively. The total length of the cell is $L + 2r$. (Others have used L to indicate total cell length.) The first subscript (0 or α) indicates the initial value or the value at any particular age, α, and the second subscript indicates the location, either the cylinder (cy), the old pole (op), the new pole (np), or the total (tot) cell. The height of the new pole, h, is measured from the end of the cylinder toward the leading edge of the newly forming poles. At division, $h = r$. The start of invagination or constriction takes place at time T_c.

For an exponential increase in volume,

$$V_{\alpha_{tot}} = 2^{\alpha} V_{0_{tot}} \tag{1}$$

At any time, α, during the division cycle, the total volume of the cell is the sum of the volume of the cylindrical portion, the old pole volume, and any new pole synthesized. By substitution and rearrangement, and from the formula for the volume of a cylinder, one can obtain the length of the cylinder at time α. From the formulas for the area of the cylinder, volumes of the new and old poles, and the total cell volume, one can find the area of the cylinder at any time during the division cycle. Then, from the formulas for the areas of the old and new poles and considering that the total area of the cell is the sum of the area of the cylindrical portion and the old and new poles, a formula for the total cell area can be produced

$$A_{\alpha_{tot}} = \frac{2}{r}\left\{2^{\alpha}\left(\frac{4}{3}\pi r^3 + \pi r^2 L\right) - \frac{4}{3}\pi r^3 - \left[\frac{4}{3}\pi r^3 - \frac{2}{3}\pi\left((r - h_\alpha)^2(2r + h_\alpha)\right)\right]\right\} + 4\pi r^2 + 4\pi r h_\alpha \tag{2}$$

which by rearrangement and reduction gives

$$A_{\alpha_{tot}} = \frac{8}{3}(2^{\alpha})\pi r^2 + 2(2^{\alpha})\pi r L + \frac{4}{3}\pi r^2 + \frac{4}{3}\pi\frac{h_\alpha{}^3}{r} \tag{3}$$

Since cell constriction starts at age T_c, and the new pole area increases at a constant rate during the remaining time of the division cycle, the height of the new pole during the division cycle is given by

$$h_\alpha = 0, \text{ when } 0 \le \alpha \le T_c \tag{4}$$

and

$$h_\alpha = r\left(\frac{\alpha - T_c}{1 - T_c}\right), \text{ when } T_c < \alpha \le 1.0 \tag{5}$$

From the height of the new poles and the formula for the area of the cell, differentiation with respect to time gives the rate of area increase during the division cycle:

$$\left(\frac{dA}{d\alpha}\right)_{0<\alpha<1.0} = \frac{8}{3}(2^{\alpha})\ln 2\pi r^2 + 2(2^{\alpha})\ln 2\pi L + \frac{4}{r}\pi\left[h_\alpha{}^2\left(\frac{r}{1 - T_c}\right)\right] \tag{6}$$

For the exponential increase in mass during the division cycle,

$$M_\alpha = 2^{\alpha} M_{0_{tot}} \tag{7}$$

Differentiating mass with respect to α, we get

$$\frac{dM}{d\alpha} = 2^{\alpha}\ln 2 M_{0_{tot}} \tag{8}$$

Dividing equation 6 by equation 8, we get the ratio of the differential rate of increase of the area to the differential rate of increase in mass,

$$\left(\frac{dA}{dM}\right)_{0<\alpha\le1.0} = \frac{8\pi r^2}{3M_{0_{tot}}} + \frac{2\pi L}{M_{0_{tot}}} + \frac{4\pi h_\alpha{}^2}{\ln 2\ 2^{\alpha}\ M_{0_{tot}}(1 - T_c)} \tag{9}$$

This equation can be simplified by dividing through by the first two terms so that

$$\left(\frac{dA}{dM}\right)_{0<\alpha\le1} = 1 + \frac{6h_\alpha{}^2}{2^{\alpha}\ln 2(1 - T_c)(4r^2 + 3L)} \tag{10}$$

A cell growing in steady-state conditions has a given initial and constant radius, an initial cylindrical wall length, and a time for the

start of initiation during the cycle. By combining these in a new constant, κ, an equation can be obtained

$$\left(\frac{dA}{dM}\right)_{0\le\alpha\le1} = 1 + \kappa\left(\frac{h_\alpha^2}{2^\alpha}\right) \quad (11)$$

which indicates that the rate of increase of the cell wall, compared with the rate of mass increase, is constant before constriction (as $h_\alpha = 0$) and increases after the start of constriction as the square of the height of the new poles and inversely as 2 to the cell age.

Caveats and generalizations. Although a precise model has been presented here based on a simple geometrical analog of the cell shape, it should be emphasized that the data do not yet allow one to differentiate between this model and many other equally likely models. For example, the cell may not be a cylinder with hemispherical ends; there may be bulges, and the shape of the poles may be more complex. Also, the new poles may not grow by adding equal areas in equal times but by other modes of increase. Nevertheless, the important point is that even if the actual model is different than the one presented here, it will still be true that the cell density does not have to change during the cycle and that there will be an increase in the ratio of area increase to mass increase during invagination. Whether the model proposed here can ever be differentiated from other very similar models by any reasonable experimental procedure or measurement is a question which is difficult to answer now. It should be noted that the main idea, that the cell surface increases to accommodate the synthesized mass of the cell, explains the experimental results.

ACKNOWLEDGMENTS

This work was supported by grant DMB 8417403 A01 from the National Science Foundation.

I thank Ming-Lin Hsieh for her diligent and conscientious performance of the experiments, Michael Savageau for his encouragement during periods of mathematical blockage, and Arthur Koch for his comments. Alexandra Cooper worked on the editing of this paper and made it much clearer than it would have otherwise been.

LITERATURE CITED

1. **Aldea, M., E. Herrero, and F. J. Trueba.** 1982. Constancy of diameter through the cell cycle of *Salmonella typhimurium* LT2. Curr. Microbiol. **7**:165–168.
2. **Begg, K. J., and W. D. Donachie.** 1977. Growth of the *Escherichia coli* cell surface. J. Bacteriol. **129**:1524–1536.
3. **Burdett, I. D. J., and T. B. L. Kirkwood.** 1983. How does a bacterium grow during its cell cycle? J. Theor. Biol. **103**:11–20.
4. **Burdett, I. D. J., and R. G. E. Murray.** 1974. Electron microscope study of septum formation in *Escherichia coli* strains B and B/r during synchronous growth. J. Bacteriol. **119**:1039–1056.
5. **Burman, L. G., J. Raichler, and J. T. Park.** 1983. Evidence for diffuse growth of the cylindrical portion of the *Escherichia coli* murein sacculus. J. Bacteriol. **155**:983–988.
6. **Chaloupka, J., and M. Strnadovà.** 1972. Turnover of murein in a diaminopimelic acid dependent mutant of *Escherichia coli*. Folia Microbiol. **17**:446–455.
7. **Collins, J., and M. Richmond.** 1962. Rate of growth of *Bacillus cereus* between divisions. J. Gen. Microbiol. **28**:15–33.
8. **Cooper, S.** 1969. Cell division and DNA replication following a shift to a richer medium. J. Mol. Biol. **43**:1–11.
9. **Cooper, S., and C. E. Helmstetter.** 1968. Chromosome replication and the division cycle of *Escherichia coli*. J. Mol. Biol. **31**:519–540.
10. **Cooper, S., and N. Metzger.** 1986. Efficient and quantitative incorporation of diaminopimelic acid into the peptidoglycan of *Salmonella typhimurium*. FEMS Microbiol. Lett. **36**:191–194.
11. **Cooper, S., and T. Ruettinger.** 1973. Replication of deoxyribonucleic acid during the division cycle of *Salmonella typhimurium*. J. Bacteriol. **114**:966–973.
12. **Cullum, J., and M. Vicente.** 1978. Cell growth and length distribution in *Escherichia coli*. J. Bacteriol. **134**:330–337.
13. **Donachie, W. D., and K. J. Begg.** 1970. Growth of the bacterial cell. Nature (London) **227**:1220–1224.
14. **Donachie, W. D., K. J. Begg, and M. Vincente.** 1976. Cell length, cell growth and cell division. Nature (London) **264**:328–333.
15. **Donachie, W. D., N. C. Jones, and R. Teather.** 1973. The bacterial cell cycle. Symp. Soc. Gen. Microbiol. **23**:9–44.
16. **Driehuis, F., and J. T. M. Wouters.** 1985. Effect of diaminopimelic acid-limited growth on the peptidoglycan composition of *Escherichia coli* W7. Antonie van Leeuwenhoek J. Microbiol. **51**:556.
17. **Ecker, R. E., and G. Kokaisl.** 1969. Synthesis of protein, ribonucleic acid, and ribosomes by individual bacterial cells in balanced growth. J. Bacteriol. **98**:1219–1226.
18. **Goodell, E. W.** 1985. Recycling of murein by *Escherichia coli*. J. Bacteriol. **163**:305–310.
19. **Goodell, E. W., and U. Schwarz.** 1985. Release of cell wall peptides into culture medium by exponentially growing *Escherichia coli*. J. Bacteriol. **162**:391–397.
20. **Grover, N. B., C. L. Woldringh, A. Zaritsky, and R. F. Rosenberger.** 1977. Elongation of rod-shaped bacteria. J. Theor. Biol. **67**:181–193.
21. **Harvey, R. J., A. G. Marr, and P. R. Painter.** 1967. Kinetics of growth of individual cells of *Escherichia coli* and *Azotobacter agilis*. J. Bacteriol. **93**:605–617.
22. **Helmstetter, C. E.** 1967. Rate of DNA synthesis during the division cycle of *E. coli* B/r. J. Mol. Biol. **24**:417–427.
23. **Helmstetter, C. E., and S. Cooper.** 1968. DNA synthesis during the division cycle of rapidly growing *E. coli* B/r. J. Mol. Biol. **31**:507–518.
24. **Hoffman, H., and M. E. Frank.** 1965. Time-lapse photomicrography of cell growth and division in *Escherichia coli*. J. Bacteriol. **89**:212–216.
25. **Hoffman, B., W. Messer, and U. Schwarz.** 1972. Regulation of polar cap formation in the life cycle of *Escherichia coli*. J. Supramol. Struct. **1**:29–37.
26. **Kjeldgaard, N. O., O. Maaløe, and M. Schaechter.** 1958. The transition between different physiological states during balanced growth of *Salmonella typhimurium*. J. Gen. Microbiol. **19**:607–616.
27. **Koch, A. L.** 1982. On the growth and form of *Escherichia coli*. J. Gen. Microbiol. **128**:2527–2539.
28. **Koch, A. L.** 1983. The surface stress theory of microbial morphogenesis. Adv. Microb. Physiol. **24**:301–366.
29. **Koch, A. L.** 1983. The shapes of gram-negative organisms: variable-T models, p. 99–104. *In* R. Hakenbeck, J.-V. Höltje, and H. Labischinski (ed.), The target of penicillin. Walter de Gruyter & Co., Berlin.
30. **Koch, A. L.** 1985. Bacterial wall growth and division or life without actin. Trends Biochem. Sci. **10**:11–14.
31. **Koch, A. L.** 1985. How bacteria grow and divide in spite of internal hydrostatic pressure. Can. J. Microbiol. **31**:1071–1084.
32. **Koch, A. L., and G. Blumberg.** 1976. Distribution of bacteria in the velocity gradient centrifuge. Biophys. J. **16**:389–405.
33. **Koch, A. L., and I. D. J. Burdett.** 1984. The variable T model for gram-negative morphology. J. Gen. Microbiol. **130**:2325–2338.
34. **Koch, A. L., and H. R. Levy.** 1955. Protein turnover in growing cultures of *Escherichia coli*. J. Biol. Chem. **217**:947–957.
35. **Koch, A. L., and M. Schaechter.** 1962. A model for the statistics of the cell division process. J. Gen. Microbiol. **29**:435–454.
36. **Koch, A. L., R. W. H. Verwer, and N. Nanninga.** 1982. Incorporation of diaminopimelic acid into the old poles of *Escherichia coli*. J. Gen. Microbiol. **128**:2893–2898.
37. **Koppes, L. J. H., and N. Nanninga.** 1980. Positive correlation between size at initiation of chromosome replication in *Escherichia coli* and size at initiation of cell constriction. J. Bacteriol. **143**:89–99.
38. **Koppes, L. J. H., N. Overbeeke, and N. Nanninga.** 1978. DNA replication pattern and cell wall growth in *Escherichia coli* PAT 84. J. Bacteriol. **133**:1053–1061.
39. **Koppes, L. J. H., C. L. Woldringh, and N. Nanninga.** 1978. Size variations and correlation of different cell cycle events in slow-growing *Escherichia coli*. J. Bacteriol. **134**:423–433.
40. **Kubitschek, H. E.** 1970. Evidence for the generality of linear cell

growth. J. Theor. Biol. **28**:15–29.
41. **Kubitschek, H. E.** 1981. Bilinear cell growth of *Escherichia coli*. J. Bacteriol. **148**:730–733.
42. **Kubitschek, H. E.** 1986. Increase in cell mass during the division cycle of *Escherichia coli* B/r A. J. Bacteriol. **168**:613–618.
43. **Kubitschek, H. E., W. W. Baldwin, and R. Graetzer.** 1983. Buoyant density constancy during the cell cycle of *Escherichia coli*. J. Bacteriol. **155**:1027–1032.
44. **Kubitschek, H. E., W. W. Baldwin, S. J. Schroeter, and R. Graetzer.** 1984. Independence of buoyant cell density and growth rate in *Escherichia coli*. J. Bacteriol. **158**:296–299.
45. **Kubitschek, H. E., and C. L. Woldringh.** 1983. Cell elongation and division probability during the *Escherichia coli* growth cycle. J. Bacteriol. **153**:1379–1387.
46. **Lin, E. C. C., Y. Hirota, and F. Jacob.** 1971. On the process of cellular division in *Escherichia coli*. VI. Use of a methocel-autoradiographic method for the study of cellular division in *Escherichia coli*. J. Bacteriol. **108**:375–385.
47. **Loeb, A., B. E. McGrath, J. M. Navre, and O. Pierucci.** 1978. Cell division during nutritional upshifts of *Escherichia coli*. J. Bacteriol. **136**:631–637.
48. **Margolis, S., and S. Cooper.** 1971. Simulation of bacterial growth, cell division and DNA synthesis. Comput. Biomed. Res. **4**:427–443.
49. **Marr, A. G., R. J. Harvey, and W. C. Trentini.** 1966. Growth and division of *Escherichia coli*. J. Bacteriol. **91**:2388–2389.
50. **Martínez-Salas, E., J. A. Martín, and M. Vicente.** 1981. Relationship of *Escherichia coli* density to growth rate and cell age. J. Bacteriol. **147**:97–100.
51. **Meyer, M., M. A. de Jong, R. Demets, and N. Nanninga.** 1979. Length growth of two *Escherichia coli* B/r substrains. J. Bacteriol. **138**:17–23.
52. **Nanninga, N., and C. L. Woldringh.** 1985. Cell growth, genome duplication, and cell division, p. 259–318. *In* N. Nanninga (ed.), Molecular cytology of *Escherichia coli*. Academic Press, Inc., New York.
53. **Nanninga, N., C. L. Woldringh, and L. J. H. Koppes.** 1982. Growth and division of *Escherichia coli*, p. 225–270. *In* C. Nicolini (ed.), Cell growth. Plenum Publishing Corp., New York.
54. **Olijhoek, A. J. M., S. Klencke, E. Pas, N. Nanninga, and U. Schwarz.** 1982. Volume growth, murein synthesis, and murein cross-linkage during the division cycle of *Escherichia coli* PA-3092. J. Bacteriol. **152**:1248–1254.
55. **Pierucci, O.** 1978. Dimensions of *Escherichia coli* at various growth rates: model for envelope growth. J. Bacteriol. **135**: 559–574.
56. **Previc, E. P.** 1970. Biochemical determination of bacterial morphology and the geometry of cell division. J. Theor. Biol. **27**:471–497.
57. **Pritchard, R. H.** 1974. On the growth and form of a bacterial cell. Philos. Trans. R. Soc. Lond. B Biol. Sci. **267**:303–336.
58. **Rosenberger, R. F., N. B. Grover, A. Zaritsky, and C. L. Woldringh.** 1978. Control of microbial surface-growth by density. Nature (London) **271**:244–245.
59. **Rosenberger, R. F., N. B. Grover, A. Zaritsky, and C. L. Woldringh.** 1978. Surface growth in rod-shaped bacteria. J. Theor. Biol. **73**:711–721.
60. **Ryter, A., Y. Hirota, and U. Schwarz.** 1973. Process of cellular division in *Escherichia coli*; growth pattern of *E. coli* murein. J. Mol. Biol. **78**:185–195.
61. **Sargent, M. G.** 1975. Control of cell length in *Bacillus subtilis*. J. Bacteriol. **123**:7–19.
62. **Sargent, M. G.** 1978. Surface extension and the cell cycle in prokaryotes. Adv. Microb. Physiol. **18**:105–176.
63. **Schaechter, M., J. P. Williamson, J. R. Hood, Jr., and A. L. Koch.** 1962. Growth, cell and nuclear divisions in some bacteria. J. Gen. Microbiol. **29**:421–434.
64. **Schwarz, U., A. Ryter, A. Rambach, R. Hellio, and Y. Hirota.** 1975. Process of cellular division in *Escherichia coli*: differentiation of growth zones in the sacculus. J. Mol. Biol. **98**:749–759.
65. **Skarstad, K., H. B. Steen, and E. Boye.** 1985. *Escherichia coli* DNA distributions measured by flow cytometry and compared with theoretical computer simulations. J. Bacteriol. **163**:661–668.
66. **Trueba, F. J., O. M. Neijssel, and C. L. Woldringh.** 1982. Generality of the growth kinetics of the average individual cell in different bacterial populations. J. Bacteriol. **150**:1048–1055.
67. **Trueba, F. J., and C. L. Woldringh.** 1980. Changes in cell diameter during the division cycle of *Escherichia coli*. J. Bacteriol. **142**:869–878.
68. **Van Tubergen, R. P., and R. B. Setlow.** 1961. Quantitative radioautographic studies on exponentially growing cultures of *Escherichia coli*. The distribution of parental DNA, RNA, protein and cell wall among progeny cells. Biophys. J. **1**:589–625.
69. **Verwer, R. W. H., and N. Nanninga.** 1980. Pattern of *meso*-DL-2,6-diaminopimelic acid incorporation during the division cycle of *Escherichia coli*. J. Bacteriol. **144**:327–336.
70. **Woldringh, C. L., N. B. Grover, R. F. Rosenberger, and A. Zaritsky.** 1980. Dimensional rearrangement of rod-shaped bacteria following nutritional shift-up. II. Experiments with *Escherichia coli* B/r. J. Theor. Biol. **86**:441–454.
71. **Woldringh, C. L., P. Huls, E. Pas, G. J. Brakenhoff, and N. Nanninga.** 1987. Topography of peptidoglycan synthesis during elongation and polar cap formation in a cell division mutant of *Escherichia coli* MC4100. J. Gen. Microbiol. **133**:575–586.
72. **Zaritsky, A.** 1975. On dimensional determination of rod-shaped bacteria. J. Theor. Biol. **54**:243–248.
73. **Zaritsky, A., N. B. Grover, J. Naaman, C. L. Woldringh, and R. F. Rosenberger.** 1982. Growth and form in bacteria. Comments Mol. Cell. Biol. **1**:237–260.